Cdc42 and Par6–PKCζ regulate the spatially localized association of Dlg1 and APC to control cell polarization

Sandrine Etienne-Manneville,[1,5] Jean-Baptiste Manneville,[3,5] Sarah Nicholls,[1] Michael A. Ferenczi,[3,4] and Alan Hall[1,2]

[1]Medical Research Council Laboratory for Molecular Cell Biology and Cell Biology Unit, Cancer Research UK Oncogene and Signal Transduction Group and [2]Department of Biochemistry and Molecular Biology, University College London, London WC1E 6BT, England, UK
[3]National Institute for Medical Research, London NW7 1AA, England, UK
[4]Department of Biomedical Sciences, Imperial College, London SW7 2AZ, England, UK
[5]Institut Curie, Centre National de la Recherche Scientifique, UMR144, Paris 75248, cedex 05, France

Cell polarization is essential in a wide range of biological processes such as morphogenesis, asymmetric division, and directed migration. In this study, we show that two tumor suppressor proteins, adenomatous polyposis coli (APC) and Dlg1-SAP97, are required for the polarization of migrating astrocytes. Activation of the Par6–PKCζ complex by Cdc42 at the leading edge of migrating cells promotes both the localized association of APC with microtubule plus ends and the assembly of Dlg-containing puncta in the plasma membrane. Biochemical analysis and total internal reflection fluorescence microscopy reveal that the subsequent physical interaction between APC and Dlg1 is required for polarization of the microtubule cytoskeleton.

Introduction

In scratch-induced migration assays using cell monolayers, Cdc42, which is a small Rho family GTPase, is required to polarize both the actin and microtubule cytoskeletons such that cells migrate in a direction that is perpendicular to the scratch. Cell polarization involves reorientation of the Golgi apparatus, centrosome, and the associated microtubule network along the axis of migration. In primary rat astrocytes, Cdc42 mediates its effects on the microtubule cytoskeleton through spatially restricted activation of a Par6–PKCζ complex at the leading edge (Etienne-Manneville and Hall, 2001). This same complex has been implicated in numerous other polarity pathways, including asymmetric division, epithelial junction assembly, and neuronal morphogenesis (for review see Henrique and Schweisguth, 2003; Macara, 2004). In migrating astrocytes, the activation of atypical PKCζ leads to phosphorylation and inactivation of GSK-3β, which causes the adenomatous polyposis coli (APC) tumor suppressor protein to associate with microtubule plus ends at the leading edge (Etienne-Manneville and Hall, 2003). To explore how this leads to the establishment of cell polarity, we have focused on another tumor suppressor gene product, Dlg1 (hDlg and SAP97), that is an orthologue of *Drosophila melanogaster* discs large protein, which is involved in the establishment of epithelial polarity (Woods et al., 1996). Dlg1 binds to the carboxy-terminal end of APC via its PDZ domains (Matsumine et al., 1996) and colocalizes with APC in cell protrusions (Iizuka-Kogo et al., 2005), but the functional significance of this interaction is unknown.

Correspondence to Alan Hall: alan.hall@ucl.ac.uk

Abbreviations used in this paper: APC, adenomatous polyposis coli; TIRF, total internal reflection fluorescence.

The online version of this article contains supplemental material.

Results and discussion

APC binds to Dlg1 at the leading edge of migrating cells

We have previously shown that the association of APC with microtubule plus ends at the leading edge is essential for the polarization of migrating astrocytes (Etienne-Manneville and Hall, 2003). To examine whether Dlg associates with APC under these conditions, Dlg1 was first immunoprecipitated from confluent, nonmigrating primary astrocytes, but no APC could be detected in Western blot analysis (Fig. 1 A, 0 h). In contrast, within 1 h after scratch-induced cell migration, APC could be coimmunoprecipitated with Dlg1 (Fig. 1 A, 1 and 4 h). APC and Dlg1 were not detectable after immunoprecipitation with an irrelevant antibody (Fig. 1 A, control). Immunostaining revealed that 4 h after wounding, Dlg1 was concentrated in a punctuate pattern that is associated with the plasma membrane at the leading edge (Fig. 1 B, bottom) but is not present at the edges of confluent or just-wounded astrocytes (Fig. 1 B, top

The Journal of Cell Biology, Vol. 170, No. 6, September 12, 2005 895–901
http://www.jcb.org/cgi/doi/10.1083/jcb.200412172

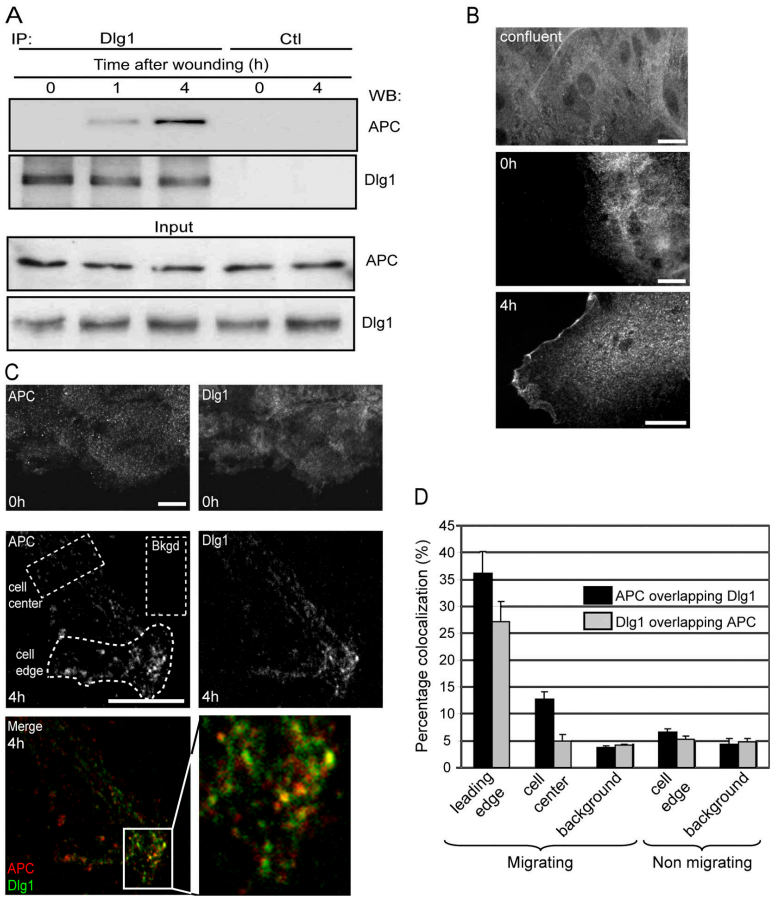

Figure 1. **Dlg1 interacts with APC at the leading edge of migrating astrocytes.** (A) Cells were lysed immediately (0 h), 1 h, or 4 h after scratching. Immunoprecipitations were performed with anti-Dlg antibodies (IP Dlg1) or control rabbit anti–mouse IgG (Ctl) and were analyzed on Western blots (WB) using anti-APC or anti-Dlg1 antibodies. Bottom panel (input) shows equal APC and Dlg1 content in different cell lysates. (B) Cells were fixed and stained before (confluent), just after (0 h), and 4 h after scratching. Localization of Dlg1 was visualized with conventional epifluorescence. (C) Costaining of Dlg1 and APC visualized by confocal microscopy 0 and 4 h after scratching. Yellow in the merged image reflects colocalization of APC (red) and Dlg1 (green) clusters (similar results were observed 8 h after wounding). Bkgd, background. Higher magnification of the boxed area (solid lines) are shown on the right. Bars, 10 μm. (D) Quantification of APC and Dlg1 colocalization. Colocalization was measured in a central region of the cell in front of the nucleus (cell center) or at the leading edge (cell edge) in migrating or nonmigrating cells. Random background colocalization was measured in front of the leading edge (background; see Materials and methods). As an example, regions that were used for quantification are shown in C (dotted lines). Error bars represent SEM.

and middle). APC accumulates as clusters on the plus ends of microtubules with the same kinetics, as previously described (Näthke et al., 1996; Etienne-Manneville and Hall, 2003). 4 h after wounding, a subset of Dlg1 puncta (26%) colocalized with APC clusters (Fig. 1, C and D). We conclude that APC and Dlg1 interact in a spatially restricted region at the leading edge of migrating cells.

Microtubule-associated APC interacts with Dlg1 puncta at the basal plasma membrane

To further investigate the relationship between microtubules APC and Dlg1, we used total internal reflection fluorescence (TIRF) microscopy. This technique illuminates only the first 200 nm above the basal plasma membrane that is in contact with the glass coverslip and, therefore, allows maximum resolution in the z-axis (for review see Toomre and Manstein, 2001). In confluent monolayers, almost no microtubules are visible by TIRF microscopy. During scratch-induced migration, microtubules can be seen in the evanescent field, but only at the front of leading edge cells (Fig. 2 A). Closer inspection of the highly elongated migrating cells reveals that microtubules are visible by TIRF only within the few microns immediately behind the leading edge (Fig. 2 A, green), whereas all microtubules are visible by conventional epifluorescence microscopy (Fig. 2 A, red). This is not caused by variations in plasma membrane substrate adherence because membrane markers and the actin cytoskeleton can be seen by TIRF microscopy throughout the protrusion and cell body (not depicted). Microtubules that are visible in the evanescent field are capped by EB1 (Fig. 2 B). We conclude that microtubule plus ends specifically associate with the basal plasma membrane at the leading edge. APC is also clearly visible within the evanescent field at the leading edge (Fig. 2 C, left). Higher magnification TIRF images show that APC clusters localize slightly forward of EB1 clusters at the plus ends of microtubules (Fig. 2 C, right) as previously described (Barth et al., 2002).

Dlg1 is not visible at the basal plasma membrane of confluent nonmigrating cells as visualized by TIRF microscopy, whereas it forms small punctate clusters that cover the basal plasma membrane at the front of the protrusion in migrating cells (Fig. 2 D). A subset of Dlg1 clusters (31.5 ± 0.1% compared with a 3.9 ± 0.6% background level) colocalize with APC-capped microtubule plus ends (Fig. 2 E, arrowheads). Some of the Dlg1 puncta at the basal plasma membrane are also found in front of microtubule plus ends (Fig. 2 E, arrows). Although actin stress fibers and cortical actin can both be visualized in the evanescence field, Dlg1 does not colocalize with these structures (Fig. 2 F). Furthermore, the inhibition of actin polymerization by cytochalasin D (1 μM) or the inhibition of microtubule dynamics by low doses of nocodazole (0.5 μM) does not affect Dlg1 recruitment at the basal plasma membrane (unpublished data).

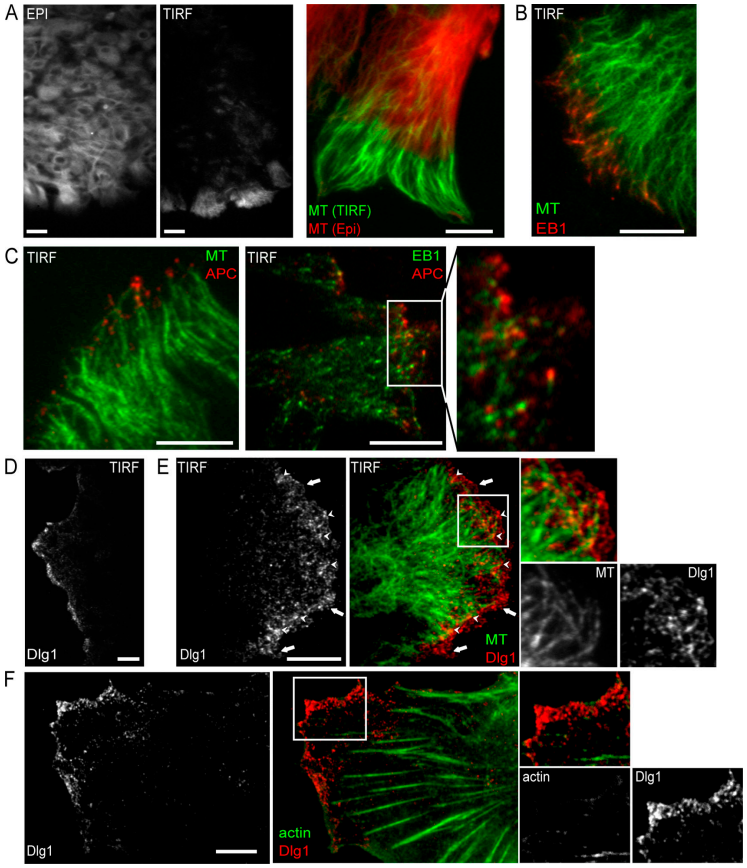

Figure 2. **Spatial organization of APC and Dlg1 at the leading edge.** (A) Organization of the microtubule cytoskeleton in a scratched monolayer of astrocytes visualized by TIRF microscopy at low (left) and high (right) resolution. Conventional epifluorescence (red) and TIRF (green) images are superimposed on the high resolution image. (B) TIRF microscopy of EB1 (red) and microtubules (green). (C) TIRF microscopy of APC (red) and microtubules (green; left) and APC (red) and EB1 (green; right). Note that APC clusters are in proximity of microtubule plus ends only at the leading edge in contrast to EB1 clusters. (D) Low and high (E) magnification TIRF images (red or white, Dlg1; green, tubulin). (E) Two pools of Dlg1 can be distinguished: one pool that is associated with microtubule tips (arrowheads) and a membrane-associated pool that is localized in front of microtubules (arrows). Bars, 10 μm; (left panels in A and D), 20 μm. (F) TIRF microscopy of Dlg1 (red; left) and actin (green; right). (C, E, and F) Higher magnifications of the boxed areas are shown on the right.

Dlg1 localization is controlled by Cdc42 and PKCζ independently of APC

To analyze the mechanism of Dlg1 recruitment, we expressed various constructs to interfere either with APC recruitment or with the association of APC and Dlg1. The carboxy-terminal region of APC comprises multiple functional domains, including a low affinity microtubule-binding site, an EB1-binding site (Matsumine et al., 1996; for review see Bienz, 2002), and a carboxy-terminal motif for binding PDZ domains in Dlg1 (Fig. 3 A). Expression of the EB1-binding domain of APC (APC–EB1) or the APC-binding domain of EB1 (EB1-bZIP) prevented the recruitment of APC to microtubule plus ends (Fig. 3, B and C) without affecting Dlg1 recruitment at the leading edge (Fig. 3 E). The microtubule-binding domain of APC or full-length EB1 had no effect on endogenous APC (Fig. 3 C). The carboxy-terminal PDZ-binding domain of APC, which inhibits APC–Dlg1 interaction in COS cells (unpublished data), does not perturb APC clustering at microtubule plus ends nor does it prevent Dlg1 recruitment at the leading edge (Fig. 3, B–E). Similarly, a mutant form of Dlg1 that cannot bind APC does not affect APC localization (Fig. 3, B and C; Dlg1-GRRF), and it localizes correctly at the leading edge (Fig. 3, D and E). These results show that APC–EB1 interaction is required for APC clustering at microtubule plus ends but that this is not required for Dlg1 localization. In agreement with this, the localization of Dlg1 has been shown to be mediated by sequences in its carboxy-terminal region (i.e., independent of its PDZ domains; Kohu et al., 2002; Massimi et al., 2003).

We have previously shown that the expression of dominant-negative Cdc42 (N17Cdc42), the amino-terminal domain of Par6c or kinase-dead PKCζ, or the addition of a PKCζ pseudosubstrate (PKCζ-PS) inhibits the association of APC with microtubule plus ends in migrating astrocytes (Etienne-Manneville and Hall, 2003). As shown in Fig. 3 (D and E), these inhibitors also prevent the formation of Dlg1 puncta in the plasma membrane at the leading edge. In contrast, the expression of a constitutively activated mutant of GSK-3β (GSK-3β S9A) has no effect on Dlg1 recruitment (Fig. 3 E), whereas it abolishes APC–microtubule association (Fig. 3 C; Etienne-Manneville and Hall, 2003). We conclude that microtubule recruitment of APC and cortical recruitment of Dlg1 are controlled by two divergent pathways that are downstream of Cdc42/Par6–PKCζ (Fig. 4 D). Furthermore, APC and Dlg1 recruitment spatially controls the subsequent PDZ-mediated association of these two proteins.

APC-Dlg1 interaction is required for astrocyte polarization

We have previously shown that the centrosome and microtubule cytoskeleton play an integral part in the polarization of migrating astrocytes (Etienne-Manneville and Hall, 2001). During scratch-induced migration, the centrosome reorients to face the direction of migration, and an elongated network of microtubules emerges from the centrosome and is directed specifically to the leading edge, where it reaches the proximity of the basal plasma membrane (Fig. 2 A).

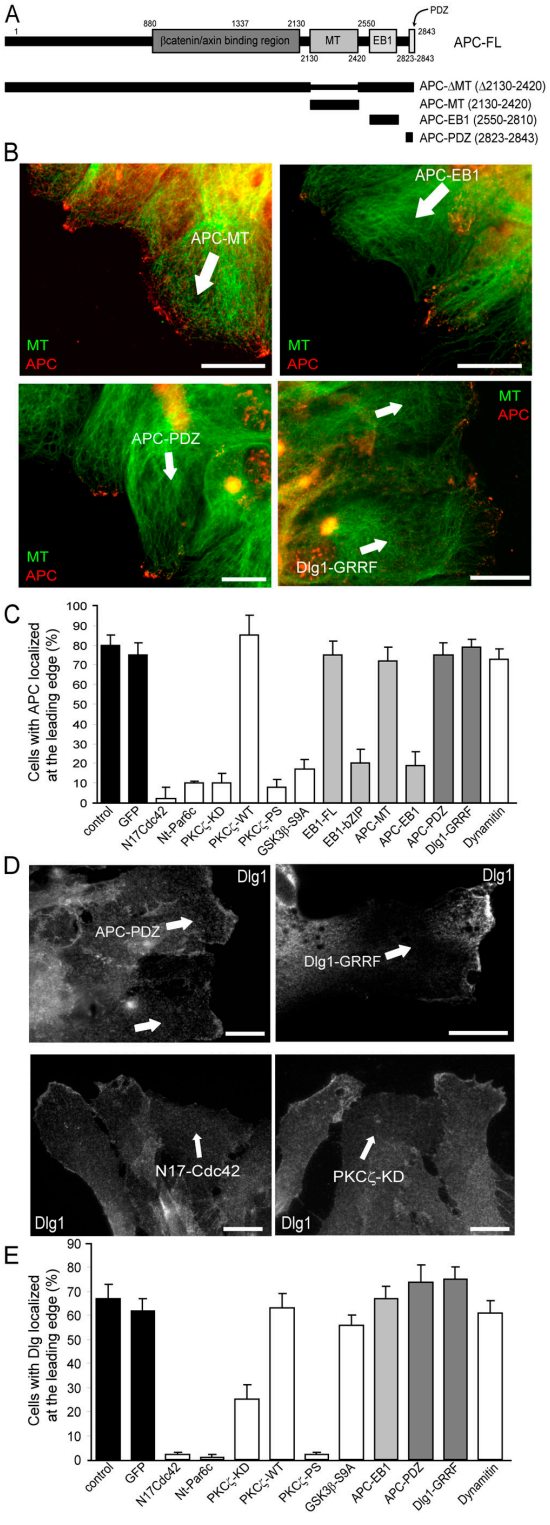

Figure 3. **A Cdc42-PKCζ–dependent, GSK-3β/APC-independent pathway controls Dlg1 localization.** (A) APC constructs that were used in this study. Astrocyte monolayers were scratched, and leading edge cells were immediately microinjected with the indicated constructs or incubated in the presence of PKCζ pseudosubstrate (PKCζ-PS; 10 μM for 1 h). Numbers correspond to the amino acid sequences of APC. (B) APC localization visualized with epifluorescence (green, tubulin; red, APC). (C) Percentage of cells with APC clusters at the leading edge. (D) Dlg1 localization visualized with epifluorescence. (B and D) 4 h after wounding, cells were fixed and stained with antibodies recognizing the microinjected constructs. Cells expressing the injected constructs are indicated by an arrow. Similar results were observed 8 h after wounding. Bars, 10 μm. (E) Percentage of cells with Dlg1 recruitment at the leading edge. (C and E) Results are means ± SEM of three independent experiments scoring at least 150 cells.

Depletion of endogenous APC by two different siRNAs (Fig. S1, available at http://www.jcb.org/cgi/content/full/jcb.200412172/DC1) strongly perturbs centrosome reorientation (Fig. 4 C). More specific inhibition of APC recruitment to microtubule plus ends by the expression of constructs or drugs (Fig. 3 C) strongly perturbs the association of microtubules with the basal plasma membrane at the leading edge of migrating cells, as visualized by TIRF microscopy (Fig. 4 A), as well as perturbs centrosome reorientation (Fig. 4, B and C) and cell migration (Fig. S2, available at http://www.jcb.org/cgi/content/full/jcb.200412172/DC1). The expression of full-length APC (APC-FL), the microtubule-binding domain of APC (APC-MT), a truncated APC lacking the microtubule-binding domain (APC-ΔMT), or full-length EB1 (EB1-FL) had no effect on microtubule anchoring or centrosome reorientation (Fig. 4, A and C). We conclude that APC clustering at microtubule plus ends is required for microtubule network polarization. The APC–EB1 interaction has similarities with Kar9p-Bim1p, which mediates cortical attachment of cytoplasmic microtubules and spindle orientation in budding yeast (Lee et al., 2000). However, whereas Kar9p recruitment is driven by the actin-associated motor Myo2p (Beach et al., 2000; Hwang et al., 2003), APC recruitment in astrocytes occurs in a region that is rather devoid of actin filaments (unpublished data), and the actin-disrupting drug cytochalasin D has no effect on microtubule organization, APC clustering at plus ends, microtubule association with the plasma membrane, or centrosome reorientation (unpublished data).

To test the role of APC–Dlg1 interaction in cell polarization, we expressed the carboxy-terminal PDZ-binding domain of APC or a mutant form of Dlg1 that cannot bind APC (Dlg1-GRRF; Ishidate et al., 2000). Although these constructs do not perturb APC clustering at microtubule plus ends or Dlg1 recruitment into puncta (Fig. 3), they strongly perturb microtubule association with the basal plasma membrane at the leading edge (as seen in TIRF; Fig. 4 A), centrosome reorientation (Fig. 4, B and C), and cell migration (Fig. S2). Loss of microtubule polarization upon disruption of the APC–Dlg1 interaction is not total, suggesting that other polarization signals such as cell–cell interactions might also make a contribution. The expression of full-length Dlg1 (Dlg1-FL) had no effect on centrosome reorientation (Fig. 4 C) or cell migration (Fig. S2). We confirmed the essential role of Dlg1 in centrosome reorientation by using siRNAs. Two different siRNAs, each cotransfected with GFP, strongly reduced Dlg expression 3 d after transfection (Fig. S1) and dramatically reduced centrosome reorientation in transfected cells (Fig. 4, B and C; Dlg1-siRNA). We conclude that the APC–Dlg1 interaction that localized at the front of the cell is essential for microtubule polarization, centrosome reorientation, and cell migration.

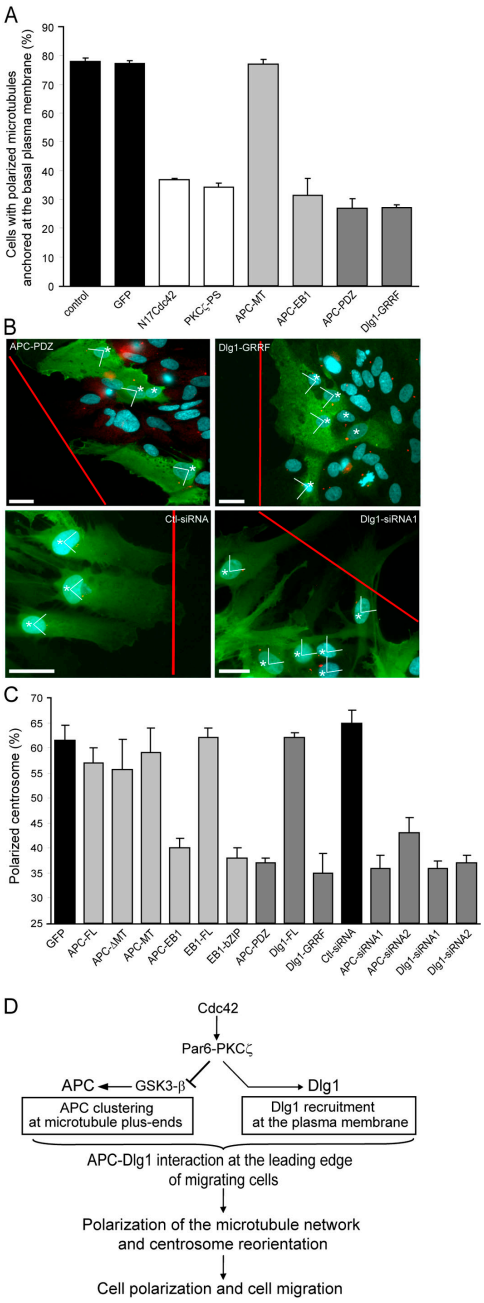

Figure 4. **APC–Dlg1 interaction is required for astrocyte polarization.** When indicated, cells were nucleofected with pEGFP and siRNA and incubated for 3 d. Monolayers were scratched, microinjected with the indicated constructs, or incubated in the presence of PKCζ pseudosubstrate (PKCζ-PS; 10 μM for 1 h). (A) Polarized microtubule anchoring at the plasma membrane was assessed in astrocytes expressing the indicated constructs. (B) 8 h after wounding, cells were fixed and stained with antibodies recognizing microinjected constructs (green cells expressing the injected constructs are indicated by asterisks), antipericentin (red), and Hoechst (blue). Red lines indicate the directions of the scratch. Bars, 10 μm. (C) Centrosome polarization was assessed in astrocytes expressing the indicated constructs. As described in Materials and methods, 25% of polarized centrosome corresponds to a random orientation. Results are means ± SEM of three independent experiments scoring at least 100 (A) or 300 (C) cells. (D) Schematic diagram showing molecular pathways occurring at the leading edge of migrating astrocytes that control APC and Dlg1 localization and subsequent microtubule polarization and cell migration.

We propose that the APC–Dlg1 interaction serves as a link between the basal plasma membrane and microtubule plus ends to promote microtubule anchoring. Microtubule anchoring may, in turn, participate in centrosome reorientation by recruiting or activating the microtubule minus end–directed dynein–dynactin motor complex, which is known to be essential (Etienne-Manneville and Hall, 2001; Palazzo et al., 2001). Indeed, Dlg1 has been reported to interact indirectly with the dynein–dynactin complex (Haraguchi et al., 2000). As previously reported in fibroblasts (Dujardin et al., 2003), we find that the dynein–dynactin complex is present at the leading edge plasma membrane of migrating astrocytes and along the extremities of membrane-captured microtubules (unpublished data). The inhibition of dynein motor function by the overexpression of dynamitin blocks centrosome reorientation (Etienne-Manneville and Hall, 2001) but does not affect APC or Dlg1 recruitment at the leading edge (Fig. 3, C and E; dynamitin). Conversely, APC–Dlg1 interaction is not required for dynein complex recruitment at the leading edge (not depicted), although it may be essential for dynein motor function.

In conclusion, we provide evidence that membrane-associated Dlg1 interacts with microtubule-bound APC to polarize the microtubule cytoskeleton during cell migration. The Par6–PKCζ complex plays a central role downstream of Cdc42 in spatially regulating both APC and Dlg1 through a bifurcating signal transduction pathway (Fig. 4 D). Dlg1 and Par6–aPKC are both involved in other polarity pathways such as epithelial cell morphogenesis; the work described in this study suggests a hierarchical biochemical connection between the two. Both APC and Dlg1 are tumor suppressor proteins (for review see Polakis, 2000; Humbert et al., 2003; Vogelstein and Kinzler, 2004), suggesting an intimate connection between the establishment of polarity and the control of proliferation.

Materials and methods

Materials

Materials were obtained from the following companies: anti–α-tubulin from Sigma-Aldrich; phalloidin-rhodamine from Molecular Probes; anti-EB1 from Transduction Labs; anti-Dlg1 from Santa Cruz Biotechnology, Inc. and Upstate Biotechnology; and anti-pericentrin from BabCO. Two different anti-APC antibodies were used for this study; anti-APC (C-20), which was obtained from Santa Cruz Biotechnology, Inc., was used for Western blotting, whereas anti-APC, which was used for immunofluorescence, was a gift from I. Näthke (University of Dundee, Dundee, Scotland, UK). Secondary antibodies were obtained from Jackson ImmunoResearch Laboratories, GF109203X was purchased from Calbiochem, and PKCζ pseudosubstrate was obtained from Biosource International. GTPases, Par6, and PKCζ constructs have been described previously (Etienne-Manneville and Hall, 2001). APC-ΔMT was obtained from I. Näthke. Other APC constructs were generated by PCR of hAPC (provided by B.M. Gumbiner, Sloan-Kettering Institute, New York, NY) and were subcloned into pRK5-myc. EB1 constructs were generated by PCR of human EB1 and were subcloned into pEGFP. Dlg1 constructs were obtained from T. Akiyama (University of Tokyo, Tokyo, Japan; Matsumine et al., 1996).

APC and Dlg1 siRNA

Four siRNA duplexes corresponding to rat APC starting at nt 3577 and 5199 (GenBank/EMBL/DDBJ accession no. D38629) and to rat Dlg1-SAP97 starting at nt 1060 and 2273 (GenBank/EMBL/DDBJ accession no. U14950) were obtained from Proligo. siRNA and pEGFP were introduced into cells by nucleofection according to the vendor's instructions (Amaxa GmbH). Cells were plated on polyornithine-coated plates or cov-

erslips, and Dlg1 expression was examined at different times (Fig. S1). Centrosome reorientation was assessed 3 d later.

Immunoprecipitation

Cells were washed with ice-cold PBS containing 1 mM orthovanadate and were lysed at 4°C in Nonidet P-40 buffer (10 mM Tris-HCl, pH 7.5, 140 mM NaCl, 1 mM orthovanadate, 1% Nonidet P-40, 2 mM PMSF, 5 mM EDTA, 20 μg/ml aprotinin, and 20 μg/ml leupeptin). Nuclei were discarded after centrifugation at 10,000 *g* for 10 min. Lysates were incubated for 2 h at 4°C with Dlg1 antibodies and protein G–Sepharose beads. Immunoprecipitates were collected and washed in Nonidet P-40 buffer. Immunoprecipitated proteins were eluted with SDS sample buffer and were analyzed by 8% SDS-PAGE.

Cell culture and scratch-induced migration

Primary rat astrocytes were prepared as described previously (Etienne-Manneville and Hall, 2001). For scratch-induced assays, cells were seeded on poly-L-ornithine–precoated coverslips or 90-mm diameter dishes and were grown in serum to confluence, and the medium was changed 16 h before scratching. Individual wounds (suitable for microinjection and immunofluorescence; ~300 μm wide) were made with a microinjection needle. Wound closure occurred ~16–24 h later. Multiple wounds (suitable for subsequent biochemical analysis) were made with an eight-channel pipette (0.1–2-μl tips) that was scratched several times across the 90-mm dish. Nuclear microinjections in the first row of wound edge cells were performed immediately after scratching. Expression vectors were used at 100–200 μg/ml, and cells were stained as described previously (Etienne-Manneville and Hall, 2001). Conventional epifluorescence images of fixed cells mounted in Mowiol were obtained on a microscope (model DM6000; Leica) equipped with a 63× NA 1.32 objective and were recorded on a CCD camera (CoolSNAP HQ; Roper Scientific) using MetaMorph software (Universal Imaging Corp.).

Dual color TIRF and confocal microscopy

The TIRF microscope that was used in this study has been previously described in detail (Manneville et al., 2003). In brief, TIRF (for review see Toomre and Manstein, 2001) was achieved at the glass slide/culture medium interface using a trapezoidal glass prism. Experiments were performed at 37°C on an upright microscope (Axioplan, Carl Zeiss MicroImaging, Inc.) that was equipped with a 100× NA 1.0 water immersion objective (Carl Zeiss MicroImaging, Inc.) and an intensified CCD camera (Remote Head Darkstar, S25 Intensifier; Photonics Science). Fluorescence was excited by either an argon ion laser (λ = 488 nm; 25 mW; Melles-Griot) or a Nd:YAG laser (λ = 532 nm; 50 mW; CrystaLaser). The angle of incidence of the excitation light was fixed to 68–70° above the critical angle $\theta_c = 61.5°$. The calculated penetration depth for the argon ion laser was d_P = 75–85 nm, and for the Nd:YAG laser, it was d_P = 85–95 nm. TIRF images were acquired by using the image analysis software Optimas 6.5 (Media Cybernetics, LP). Confocal images of fixed cells that were mounted in Mowiol were taken on a scanning confocal microscope (model LSM510 Meta; Carl Zeiss MicroImaging, Inc.) with a 40× NA 1.3 oil immersion objective (Carl Zeiss MicroImaging, Inc.).

Image quantification

Colocalization of Dlg1 and APC puncta or Dlg1 and microtubules was quantified by using the measure colocalization function within the Metamorph software. Images were first filtered by using the flatten background function. Colocalization was quantified in a 5-μm–wide region that was drawn in different areas of the cells. Background colocalization was estimated by measuring colocalization in a region that was devoid of cells located in front of the wound edge.

Polarized microtubule anchoring at the plasma membrane was assessed by TIRF microscopy 8 h after wounding in cells that were stained with antitubulin antibody. Cells showing an increase in tubulin fluorescence specifically near the leading edge (Fig. 2 A) were defined as cells with polarized microtubule anchoring. Cells with microtubules randomly contacting the plasma membrane were scored as negative. At least 100 cells from three independent experiments were scored.

Centrosome reorientation was determined as described previously (Etienne-Manneville and Hall, 2001, 2003). In brief, 8 h after wounding, astrocytes were fixed and stained with antipericentrin (centrosome), Hoechst (nucleus), and anti-myc when necessary. Cells in which the centrosome was within the quadrant facing the wound were scored as positive (polarized centrosome). Random orientation of the centrosome, therefore, corresponds to a value of 25% of correctly polarized cells. For each point, at least 300 cells from three independent experiments were examined.

Online supplemental material

Fig. S1 shows Western blot analysis of Dlg1 and APC expression after siRNA transfection in astrocytes. Fig. S2 shows the effects of APC and Dlg1 constructs on astrocyte migration. Online supplemental material is available at http://www.jcb.org/cgi/content/full/jcb.200412172/DC1.

We thank I. Näthke, B.M. Gumbiner, and T. Akiyama for plasmids and reagents. We also thank D. Louvard and B. Goud (Institut Curie, Paris, France) and J.-P. Henry, E. Karatekin, and S. Huet (Institut de Biologie Physico-Chimique, Paris, France) for technical support.

This work was supported by a Marie Curie Individual Fellowship (to J.-B. Manneville), a Centre National de la Recherche Scientifique grant (to S. Etienne-Manneville), a Cancer Research UK program grant (to A. Hall), and the Medical Research Council.

Submitted: 30 December 2004
Accepted: 2 August 2005

References

Barth, A.I.M., K.A. Siemers, and W.J. Nelson. 2002. Dissecting interactions between EB1, microtubules and APC in cortical clusters at the plasma membrane. *J. Cell Sci.* 115:1583–1590.

Beach, D.L., J. Thibodeaux, P. Maddox, E. Yeh, and K. Bloom. 2000. The role of the proteins Kar9 and Myo2 in orienting the mitotic spindle of budding yeast. *Curr. Biol.* 10:1497–1506.

Bienz, M. 2002. The subcellular destinations of APC proteins. *Nat. Rev. Mol. Cell Biol.* 3:328–338.

Dujardin, D.L., L.E. Barnhart, S.A. Stehman, E.R. Gomes, G.G. Gundersen, and R.B. Vallee. 2003. A role for cytoplasmic dynein and LIS1 in directed cell movement. *J. Cell Biol.* 163:1205–1211.

Etienne-Manneville, S., and A. Hall. 2001. Integrin-mediated Cdc42 activation controls cell polarity in migrating astrocytes through PKCζ. *Cell.* 106:489–498.

Etienne-Manneville, S., and A. Hall. 2003. Cdc42 regulates GSK3 and adenomatous polyposis coli (APC) to control cell polarity. *Nature.* 421:753–756.

Haraguchi, K., K. Satoh, H. Yanai, F. Hamada, M. Kawabuchi, and T. Akiyama. 2000. The hDLG-associated protein DAP interacts with dynein light chain and neuronal nitric oxide synthase. *Genes Cells.* 5:905–911.

Henrique, D., and F. Schweisguth. 2003. Cell polarity: the ups and downs of the Par6/aPKC complex. *Curr. Opin. Genet. Dev.* 13:341–350.

Humbert, P., S. Russell, and H. Richardson. 2003. Dlg, Scribble and Lgl in cell polarity, cell proliferation and cancer. *Bioessays.* 25:542–553.

Hwang, E., J. Kusch, Y. Barral, and T.C. Huffaker. 2003. Spindle orientation in *Saccharomyces cerevisiae* depends on the transport of microtubule ends along polarized actin cables. *J. Cell Biol.* 161:483–488.

Iizuka-Kogo, A., A. Shimomura, and T. Senda. 2005. Colocalization of APC and DLG at the tip of cellular protrusions in cultured epithelial cells and its dependency on cytoskeletons. *Histochem. Cell Biol.* 123:67–73.

Ishidate, T., A. Matsumine, K. Toyoshima, and T. Akiyama. 2000. The APC-hDLG complex negatively regulates cell cycle progression from the G0/G1 to S phase. *Oncogene.* 19:365–372.

Kohu, K., F. Ogawa, and T. Akiyama. 2002. The SH3, HOOK and guanylate kinase-like domains of hDLG are important for its cytoplasmic localization. *Genes Cells.* 7:707–715.

Lee, L., J.S. Tirnauer, J. Li, S.C. Schuyler, J.Y. Liu, and D. Pellman. 2000. Positioning of the mitotic spindle by a cortical-microtubule capture mechanism. *Science.* 287:2260–2262.

Macara, I.G. 2004. Par proteins: Partners in polarization. *Curr. Biol.* 14:R160–R162.

Manneville, J.B., S. Etienne-Manneville, P. Skehel, T. Carter, D. Ogden, and M. Ferenczi. 2003. Interaction of the actin cytoskeleton with microtubules regulates secretory organelle movement near the plasma membrane in human endothelial cells. *J. Cell Sci.* 116:3927–3938.

Massimi, P., D. Gardiol, S. Roberts, and L. Banks. 2003. Redistribution of the discs large tumor suppressor protein during mitosis. *Exp. Cell Res.* 290:265–274.

Matsumine, A., A. Ogai, T. Senda, N. Okumura, K. Satoh, G.H. Baeg, T. Kawahara, S. Kobayashi, M. Okada, K. Toyoshima, and T. Akiyama. 1996. Binding of APC to the human homolog of the *Drosophila* discs large tumor suppressor protein. *Science.* 272:1020–1023.

Näthke, I.S., C.L. Adams, P. Polakis, J.H. Sellin, and W.J. Nelson. 1996. The adenomatous polyposis coli tumor suppressor protein localizes to plasma membrane sites involved in active cell migration. *J. Cell Biol.* 134:165–179.

Palazzo, A.F., H.L. Joseph, Y.J. Chen, D.L. Dujardin, A.S. Alberts, K.K. Pfister, R.B. Vallee, and G.G. Gundersen. 2001. Cdc42, dynein, and dynactin regulate MTOC reorientation independent of Rho-regulated microtubule stabilization. *Curr. Biol.* 11:1536–1541.

Polakis, P. 2000. Wnt signaling and cancer. *Genes Dev.* 14:1837–1851.

Toomre, D., and D. Manstein. 2001. Lighting up the cell surface with evanescent wave microscopy. *Trends Cell Biol.* 11:298–303.

Vogelstein, B., and K.W. Kinzler. 2004. Cancer genes and the pathways they control. *Nat. Med.* 10:789–799.

Woods, D.F., C. Hough, D. Peel, G. Callaini, and P.J. Bryant. 1996. Dlg protein is required for junction structure, cell polarity, and proliferation control in *Drosophila* epithelia. *J. Cell Biol.* 134:1469–1482.